Electronic Supplementary Information

Asymmetrically coordinated single-atom Co-N_3S/C catalyst for oxygen reduction reaction

Yuzhou Tao, Yang Yu , Lingya Yi, and Weihua Hu *

School of Materials & Energy, Southwest University, Chongqing 400715, P. R. China; Chongqing Key Laboratory of Battery Materials and Technology, Chongqing 400715, P. R. China.

E-mail: whhu@swu.edu.cn

S1. Experimental Section

Chemicals: Zinc nitrate ($Zn(NO_3)_2·6H_2O$, Aladdin, 99%), 2-methylimidazole(Aladdin, 98%), 1,10-phenanthroline monohydrate (Phen)(Aladdin, 98%), Cobalt(II) chloride($CoCl_2$, Aladdin, ≥97%), L-Cysteine(Aladdin, 99%),Carbon-supported Pt/C (20 wt.%) and Nafion (5 wt.%) were purchased from Hesen Electric Co., Ltd,methanol solution, ethanol solution were purchased from Chongqing Chuandong Chemical (Group) Co. Ltd. Deionized water 18.25 MΩ·cm was used. All reagents were of analytical grade and used as received without further purification.

Synthesis of ZIF-8: In a typical procedure, $Zn(NO_3)_2·6H2O$ (12 mmol, 3.57 g) and 2-mIm (150 mmol, 12.315 g) was dissolved in 30 mL and 70 mL methanol separately, then $Zn(NO_3)_2$ solution was poured slowly into 2-mIm solution. The mixture was stirred for 24 h at room temperature. The as-obtained white precipitate was centrifuged and washed with methanol several times and dried in vacuum at 60 °C overnight.

Synthesis of NC: ZIF-8 and 1,10-phenanthroline were mixed in a ratio of 4:1 by mass and dispersed in a solution of ethanol and deionized water in a ratio of 2:1 by volume. The mixture was magnetically stirred at room temperature for 12 h and then evaporated at 85 °C. The dried powder

was annealed under Ar at 950 °C for 2 h and then naturally cooled to room temperature. The resulting black product was named NC.

Synthesis of Co-N_3S/C: 2 mg $CoCl_2$, 4.8 mg L-cysteine, and 20 mg NC were dissolved in 5 mL of deionized water, and the pH was adjusted to 10-11 using ammonia buffer solution. The mixture was sonicated for 5 min, then stirred at room temperature for 24 h. The sample was evaporated and dried in a vacuum oven at 60 °C overnight. The dried sample was heated to 250 ℃ at 5 ℃/min under Ar atmosphere and held for 2 h, and then continued to increase to 750 ℃ at 5 ℃/min, and held at 750 ℃ for 2 h under Ar atmosphere. After cooling down to room temperature naturally, as-obtained catalyst was named as Co-N_3S/C.

Synthesis of SNC: Synthesized in the same way as the Co-N_3S/C catalyst, except that $CoCl_2$ was not added.

Synthesis of Co-N_4/C: The same method as for the Co-N_3S/C catalyst was applied for synthesizing Co-N_4/C, except for that no L-cysteine was added.

Characterizations

XRD patterns were taken on a XRD-7000 diffractometer (SHIMADZU, Japan) by using Cu Kα radiation (40 kV, 30 mA) at scan rate of 5° min^{-1}. XPS measurements were performed using an ESCALAB 250Xi system (Thermo Fisher) equipped with a monochromatized Al Kα radiation source with a 20 μm spot. SEM images were were measured on a JSM-7800F (JEOL Ltd., Japan) at 10 kV. TEM images and elemental mapping were taken by a JEM-2100 electron microscope (JEOL) with an accelerating voltage of 200 kV. High-angle annular dark field (HAADF) images were acquired at an accelerating voltage of 200 kV using a JEM ARM 200F transmission electron microscope (JEOL, Japan) instrument equipped with an aberration corrector. Sample preparation was performed by dropwise addition of ethanol dispersion to a copper micro-grid. Raman spectra were collected using a LabRAM HR Evolution (Horiba, Japan) model laser Raman spectrometer.

Electrochemical Measurement

ORR electrochemical experiments were performed using a standard three-electrode system and tested with an Autolab PGSTAT302N workstation (METROHM). The catalyst ink was prepared as follows: 2.5 mg of catalyst was dispersed in 1 mL of a mixture containing 950 μL of anhydrous ethanol and 50 μL of 5 wt.% Nafion solution, and then sonicated for 30 min. Subsequently, a certain volume of homogeneous ink was carefully added dropwise onto a polished glassy carbon disk

electrode of RRDE. The catalyst-coated disk electrode was used as the working electrode, a Hg/HgO electrode served as the reference electrode, and a graphite plate was employed as the counter electrode. The electrolyte was 0.1 M KOH, and all LSV curves were recorded by negative scanning. All potentials used in this study were corrected and reported relative to RHE. Linear scanning tests west carried out in oxygen-saturated 0.1 M KOH electrolyte at 5 mV/s at 1600 rpm. CV tests were performed at 50 mV/s. The number of electrons transferred (n) and the hydrogen peroxide yield of ORR were calculated by the following equations:

$$n = \frac{4 \times I_d}{I_d + \frac{I_r}{N}}$$

$$H_2O_2(\%) = \frac{200 \times \frac{I_r}{N}}{I_d + \frac{I_r}{N}}$$

Where I_d denotes the disk current, I_r is the ring current, and N (0.37) is the current collection efficiency of the platinum ring.

The kinetic current density J_K was calculated from the Koutecky-Levich (K-L) equation:

$$\frac{1}{J} = \frac{1}{J_K} + \frac{1}{J_L}$$

Here J is the current density experimentally obtained on the disk electrode while J_L stands for diffusion-limiting current density.

GDE test

To prepare GDE, 2 mg of catalyst was ultrasonically dispersed for 30 min in a mixed solvent containing 50 μL of 5 wt% Nafion, 150 μL of deionized water, and 1800 μL of isopropyl alcohol. The resulting ink was then uniformly sprayed onto a piece of microporous carbon paper, yielding a catalyst loading of 1 mg cm^{-2}.

Zn-Air Battery tests

The performance of Zn-air batteries loaded with catalysts was tested at room temperature. The detailed experimental procedure was as follows: 2 mg of catalyst powder was mixed with 830 μL of

isopropanol, 120 μL of deionized water and 50 μL of 5% Nafion solution. The mixture was dispersed by ultrasonication for 30 min to form a slurry. The resulting catalyst slurry was then drop-coated onto a 3 × 3 cm hydrophobic carbon paper (catalyst loading 1.0 mg cm^{-2}, coated area of 1 cm^{-2} round) as the cathode electrode and dried for 2 h at room temperature. A 3.4×8.5 cm Zn plate with a thickness of 0.5 mm was polished to remove the surface oxide layer and dried with alcohol, used as the anode electrode. The electrolyte was 6 M KOH + 0.2 M $Zn(Ac)_2$ aqueous solution. The battery performance was evaluated by the electrochemical platform CHI 760.

Calculate the specific capacity according to the following formula:

$$\text{Specific capacity} = \frac{It}{M_{Zn}}$$

where I is the discharge current (A), t is the discharge time used (s), and M_{Zn} represents the weight of zinc consumed in the discharge process (g). The results obtained were converted to values in *mA-h/g*.

Calculate the corresponding energy density according to the following formula:

$$\text{Energy density} = \frac{UIt}{M_{Zn}}$$

U is the average discharge voltage

XAFS data

XAFS data were collected on an easyXAFS300+ instrument at room temperature with overall transmission mode data acquisition through the ionization chamber. The near-side and extended-side absorption data for the element Co in the samples were processed using the software Athena, Artemis, etc. according to standard procedures and parameters.

DFT calculations

All spin-polarized density functional theory (DFT) calculations were performed with the plane-wave basis set as implemented in the Vienna Ab Initio Simulation Package (VASP 5.5.4)[1, 2], and the

electrons and ions interactions were described by the projector augmented wave (PAW) potential[3, 4]. The exchange-correlation interactions were determined by the Perdew-Burke-Ernzerhof (PBE) functional within the generalized gradient approximation (GGA)[5]. The plane wave energy cutoff of 500 eV, and the convergence criterion for the residual force and energy was set to 0.05 eV $Å^{-1}$ and 10^{-5} eV, respectively. The empirical correction in Grimme's method (DFT+D3) was used to describe the van der Waals (vdW) interactions[6]. The Brillouin region was sampled by the Monkhorst-Pack method with a 1×1×1 k-point mesh. The change in the Gibbs free energy change (ΔG) for each possible step during the electrochemical synthesis of urea was obtained using the computational hydrogen electrode (CHE) model[7, 8]. According to this model, the changes in Gibbs free energy (ΔG) for all electrochemical steps was defined as: $\Delta G = \Delta E + \Delta E_{ZPE} - T\Delta S$, where the reaction energy (ΔE) can be directly obtained by analyzing the DFT total energies. The zero-point energy difference (ΔE_{ZPE}) between the products and the reactants can be computed from the vibrational frequencies. ΔS is the change in entropy between the products and the reactants at room temperature (T = 298.15 K).

S2. Extended Figures

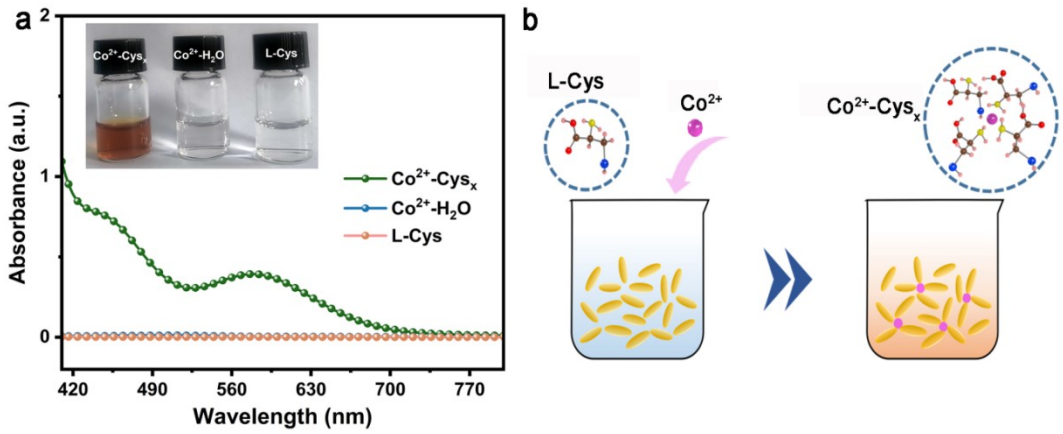

Fig. S1. a. UV spectra and optical images of Co^{2+}-Cys_x, $CoCl_2$ solution and L-Cysteine solution. b. schematic illustration of the coordinative complex formed by Co^{2+} and cysteine.

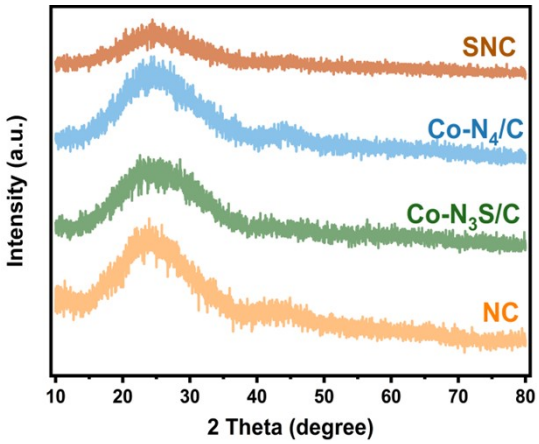

Fig. S2. XRD patterns of NC, SNC, Co-N_4/C and Co-N_3S/C.

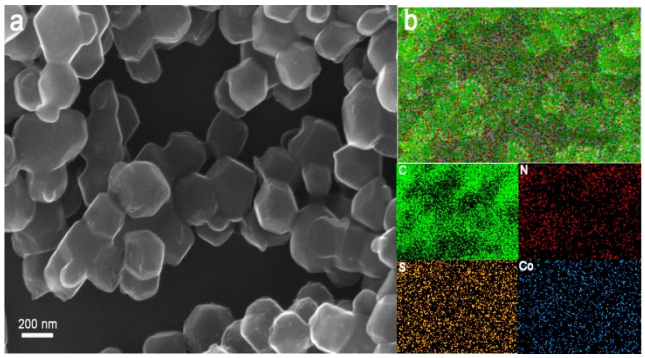

Fig. S3. SEM image and corresponding EDS mapping of Co-N_3S/C.

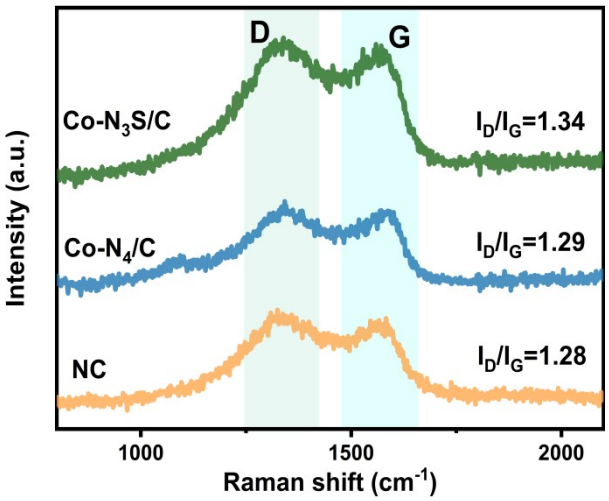

Fig. S4. Raman spectra of NC, Co-N_4/C, and Co-N_3S/C.

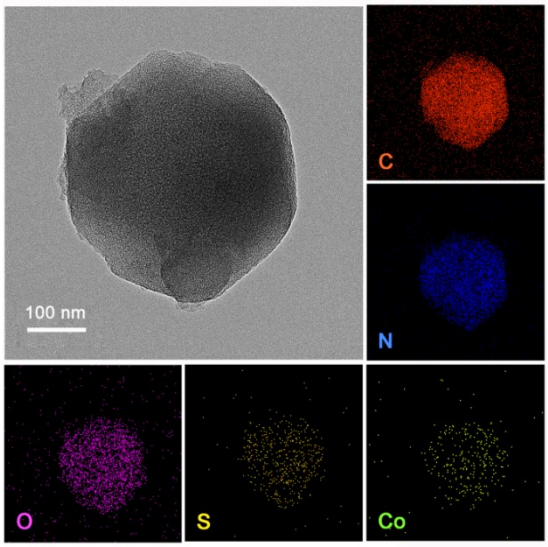

Fig. S5. TEM images of Co-N_3S/C and corresponding EDS element mapping of Co-N_3S/C catalyst.

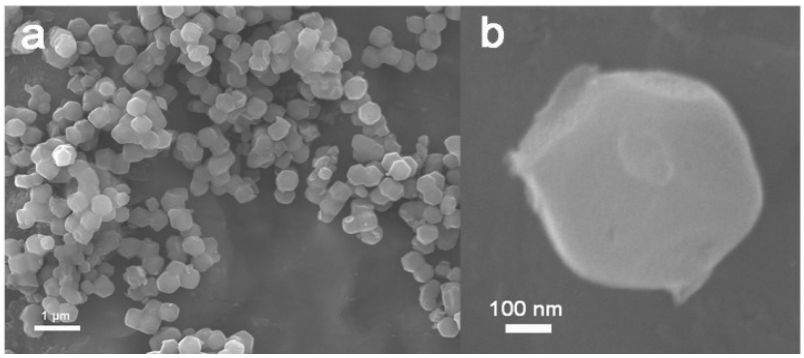

Fig. S6. SEM images of Co-N_4/C.

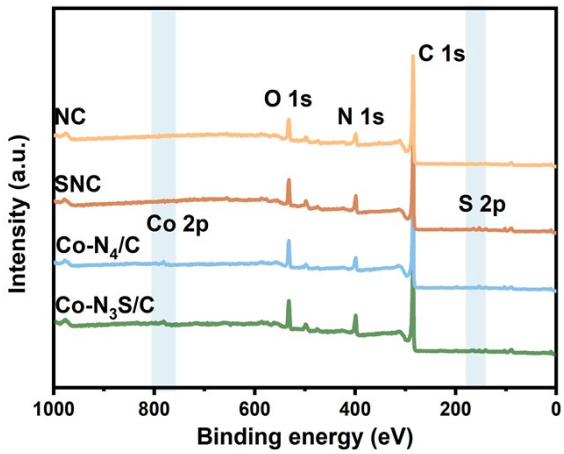

Fig. S7. XPS survey spectra of Co-N_3S/C and other catalysts.

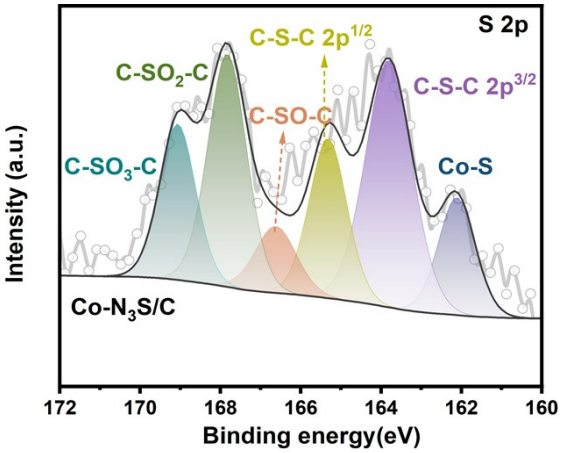

Fig. S8. XPS S 2p spectrum of Co-N_3S/C.

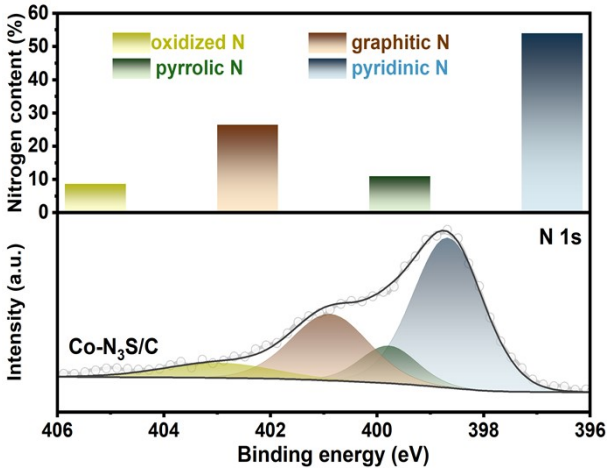

Fig. S9. XPS N 1s spectrum of Co-N_3S/C and corresponding bar charts showing the percentage of nitrogen species content.

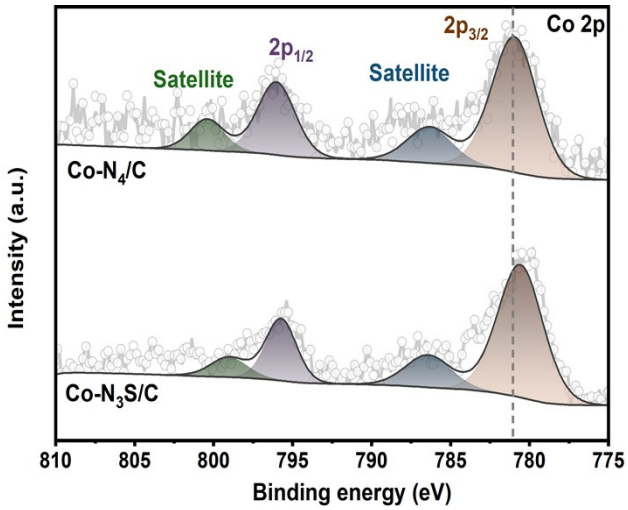

Fig. S10. XPS Co 2p spectra of Co-N_4/C and Co-N_3S/C.

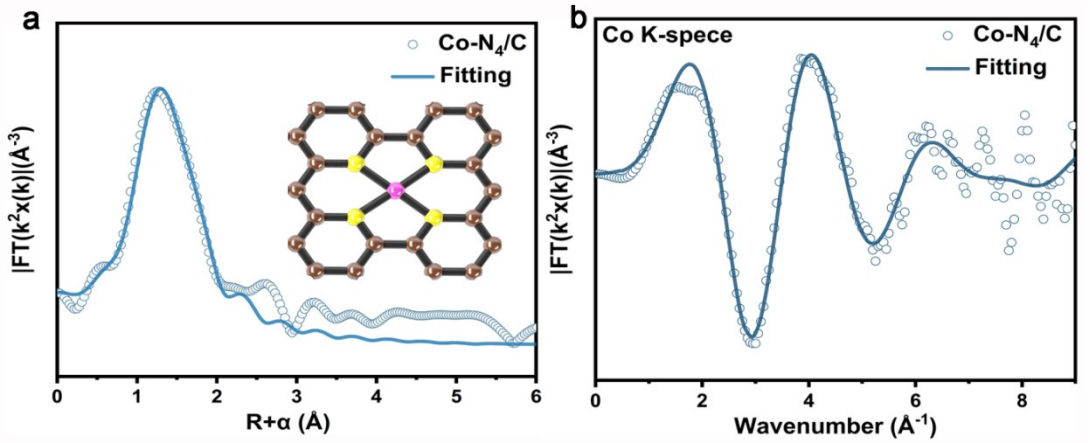

Fig. S11. a Co K-edge FT-EXAFS fitting curve of Co-N_4/C in R space; **b** K space fitting curves of Co-N_4/C.

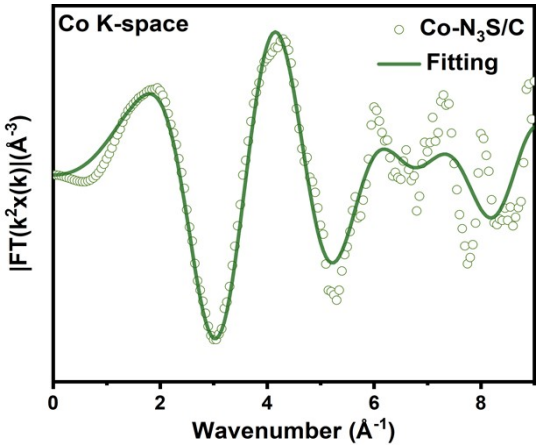

Fig. S12. K space fitting curve of Co-N_3S/C.

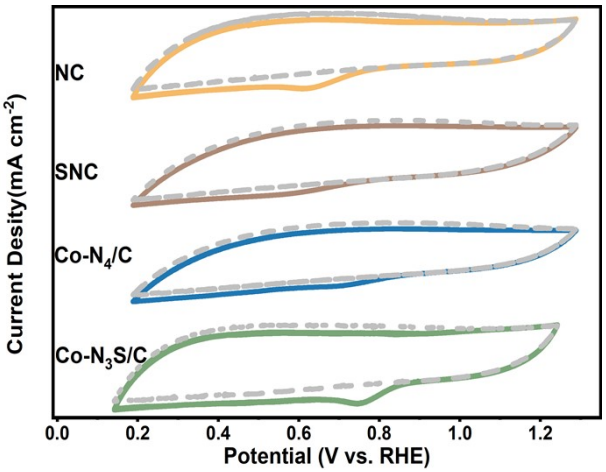

Fig. S13. CV curves of as-synthesized catalysts and Pt/C in O_2-saturated (solid line) or N-saturated (dash line) 0.1 M KOH solution.

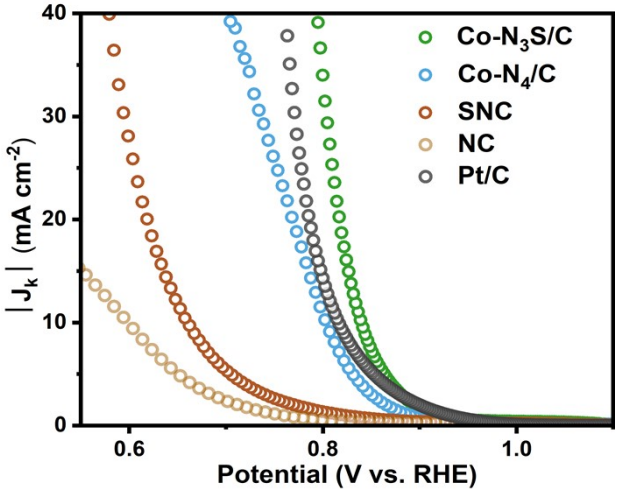

Fig. S14. $|J_k|$ of the as-synthesized catalysts and Pt/C were measured in O_2-saturated 0.1 M KOH at 1600 rpm.

.

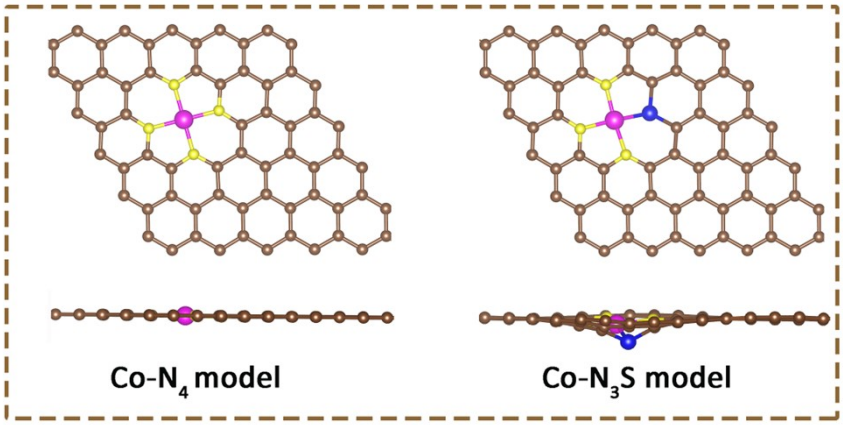

Fig. S15. Optimized atomic configurations of Co-N_4 (left) and Co-N_3S (right) model.

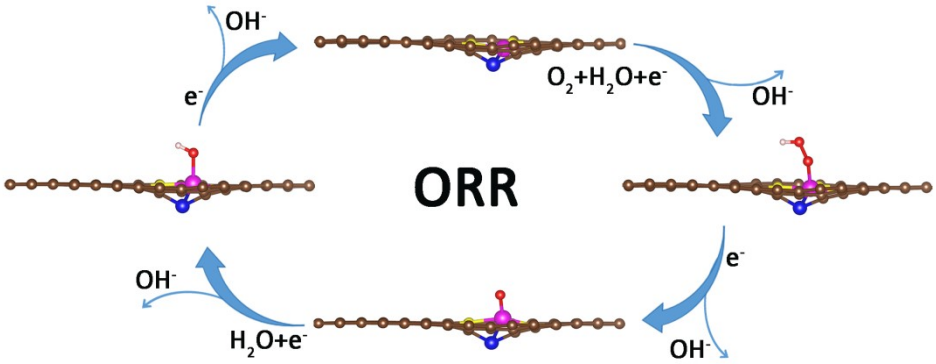

Fig. S16. Illustration of the ORR process on Co-N_3S surface.

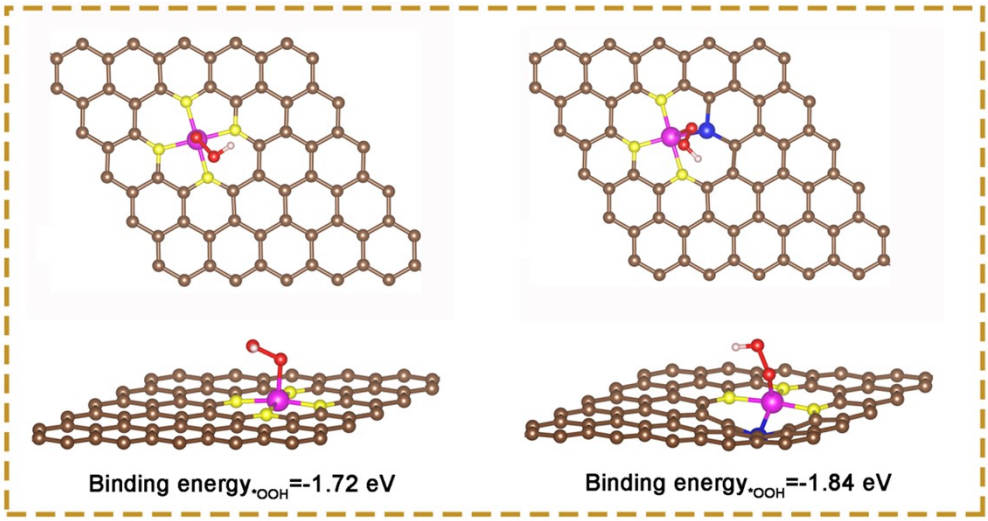

Fig. S17. Binding configurations and energies of *OOH on symmetric Co-N_4 and asymmetric Co-N_3S atomic interface models.

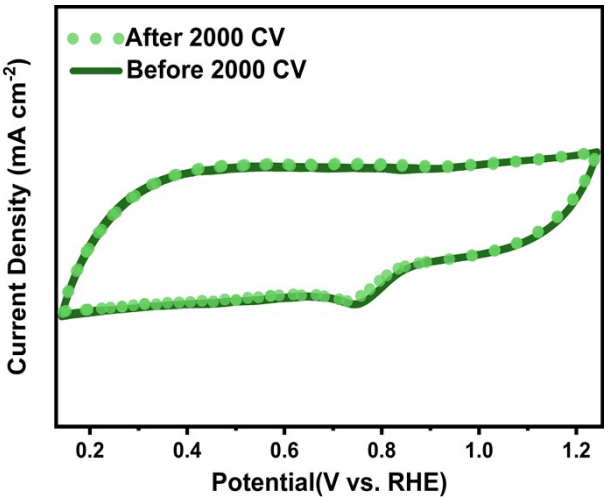

Fig. S18. CV curves of Co-N_3S/C catalyst before (solid line) and after (dash line) 2000 potential cycles in 0.1 M KOH.

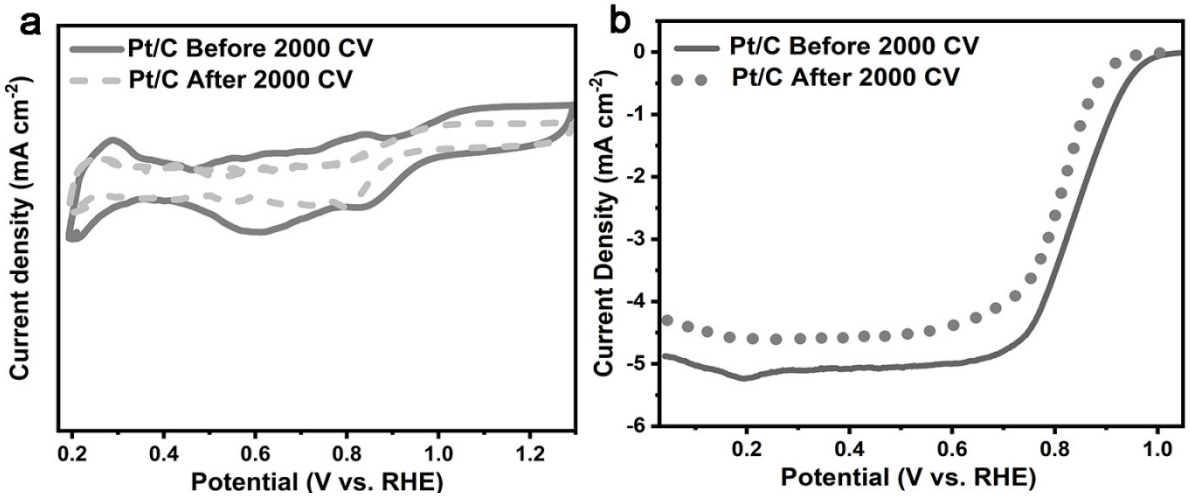

Fig. S19. CV and LSV curves of Pt/C catalyst before (solid line) and after (dash line) 2000 potential cycles in 0.1 M KOH.

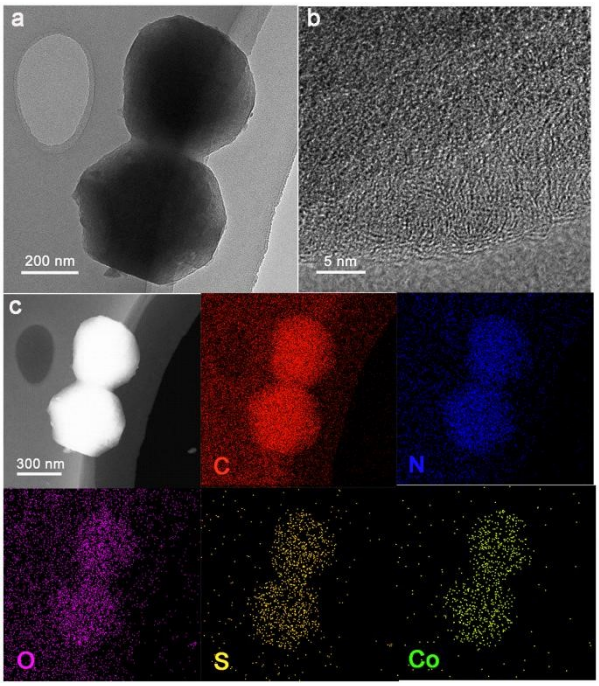

Fig. S20. a-b TEM images and HR-TEM images and **c** corresponding EDS element mapping images of Co-N_3S/C after 2000 ADT cycles in 0.1 M KOH.

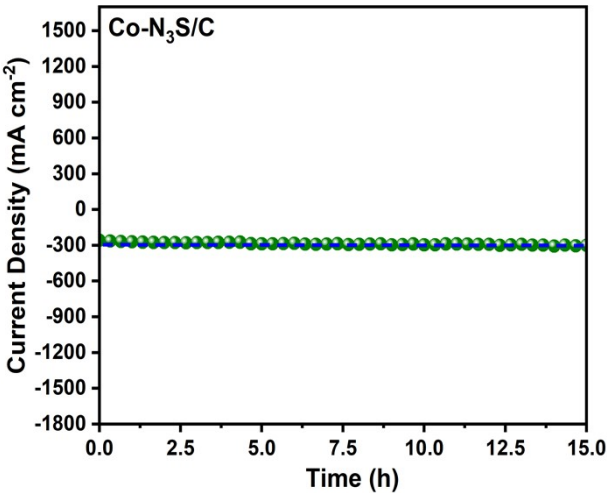

Fig. S21. i-t curve of Co-N_3S/C catalyst GDE in 1 M KOH.

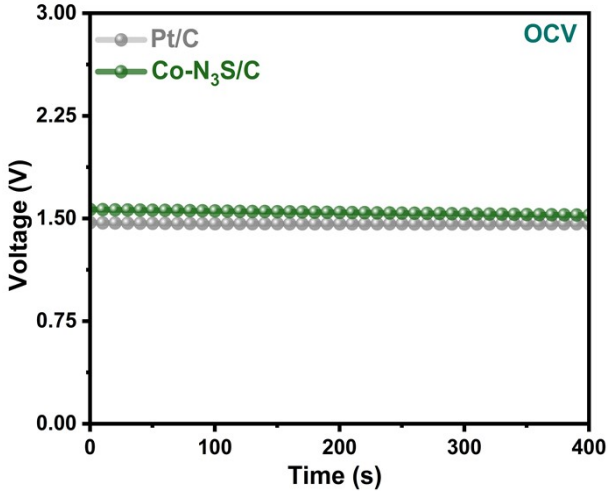

Fig. S22. OCV plots of Co-N_3S/C catalyst and Pt/C based on ZABs.

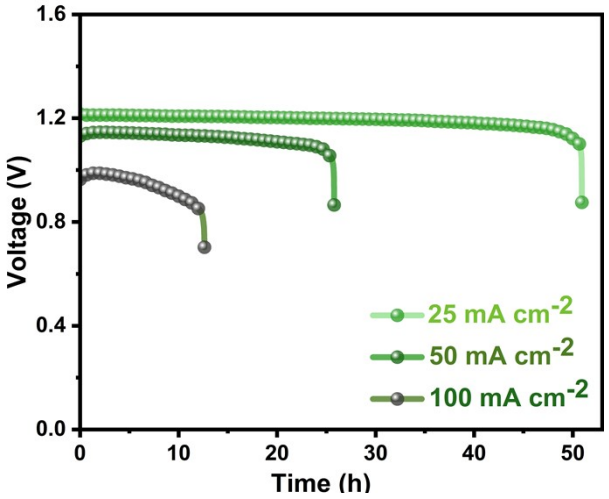

Fig. S23. Discharge profiles of Co-N_3S/C at different current densities.

S3. Tables

Table S1. Co contents of Co-N_3S/C and Co-N_4/C as measured by ICP-OES.

Sample	Co / wt.%
Co-N_4/C	3.66
Co-N_3S/C	2.76

Table S2. C、N、Co and S contents of Co-N_3S/C, Co-N_4/C, SNC, and NC as measured by XPS.

Sample	C / at.%	N / at.%	S / at.%	Co / at.%
NC	89.74	8.79	/	/

SNC	85.26	12.03	0.96	/
Co-N_4/C	88.33	10.01	/	0.77
Co-N_3S/C	83.19	13.96	0.52	0.50

Table S3. EXAFS fitting parameters at the Co K-edge of various samples.

Samples	Path	CN	R(Å)	σ^2(Å^2)	ΔE_0(eV)	R factor
Co-N_3S/C	Co-N	3.2	1.888±0.010	0.008± 0.002	-9.95	0.0150
	Co-S	0.8	2.321±0.014	0.002±0.002	-4.50	
Co-N_4/C	Co-N	2.1	2.102± 0.006	0.005±0.001	0.800	0.0058
		1.8	1.864±0.006	0.003±0.001	-9.80	

S_0^2 is the amplitude reduction factor; CN is the coordination number; R is interatomic distance (the bond length between central atoms and surrounding coordination atoms); σ^2 is Debye-Waller factor (a measure of thermal and static disorder in absorber-scatter distances); ΔE_0 is edge-energy shift. R factor is used to value the goodness of the fitting.

Table S4. The ORR performance of Co-N_3S/C catalyst reported in this paper and other catalysts recently reported in the literature. The test condition is in 0.1M KOH electrolyte.

Electrocatalysts	Onset potential (V vs. RHE)	Half-wave potential (V vs. RHE)	loading (mg cm-2)	Reference
Co-N_3S/C	0.94	0.86	0.46	This work
FeCo-NPC	0.99	0.83	0.51	[9]
CoSA-AC@SNC	0.95	0.86	0.16	[10]

Mn-CoNx/N-PC	0.97	0.85	0.25	[11]
Co-SAs/N-C/rGO	1.01	0.84	0.30	[12]
Co-S@NC	0.92	0.85	\	[13]
Co-SAs@NC	0.96	0.82	0.61	[14]
Co-SA@N-CNF	0.92	0.85	0.25	[15]
NP-Co_{SA}NC	0.94	0.86	0.16	[16]
CoNi-SAs/NC	0.88	0.76	0.4	[17]
CoN_3S_1	0.95	0.82	\	[18]
H-3DOM-Co/ONC	\	0.84	0.2	[19]
CoSA/N,S-HCS	0.96	0.85	0.12	[20]
Co2-N-HCS-900	0.99	0.86	1.00	[21]
Co2P/NP-CNTs-800	0.92	0.81	\	[22]

Reference

1. F. Shimojo, K. Hoshino and Y. Zempo, *Comput. Phys. Commun.*, 2001, **142**, 364–367.
2. G. Kresse and J. Furthmuller, *Phys. Rev. B*, 1996, **54**, 11169–11186.
3. P. E. Blochl, *Phys. Rev. B*, 1994, **50**, 17953–17979.
4. G. Kresse and D. Joubert, *Phys. Rev. B*, 1999, **59**, 1758–1775.
5. J. P. Perdew, K. Burke and M. Ernzerhof, *Phys. Rev. Lett.*, 1997, **78**, 1396–1396.
6. S. Grimme, *J. Comput. Chem.*, 2006, **27**, 1787–1799.
7. J. K. Norskov, J. Rossmeisl, A. Logadottir, L. Lindqvist, J. R. Kitchin, T. Bligaard and H. Jónsson, *J. Phys. Chem. B*, 2004, **108**, 17886–17892.
8. A. A. Peterson, F. Abild-Pedersen, F. Studt, J. Rossmeisl and J. K. Norskov, *Energy Environ. Sci.*, 2010, **3**, 1311–1315.

9. Z. Pei, H. Zhang, Y. Guo, D. Luan, X. Gu and X. W. D. Lou, *Adv Mater*, 2024, **36**, e2306047.
10. J. Rong, W. Chen, E. Gao, J. Wu, H. Ao, X. Zheng, Y. Zhang, Z. Li, M. Kim, Y. Yamauchi and C. Wang, *Small*, 2024, **20**, 2402323.
11. H. Zheng, F. Ma, H. Yang, X. Wu, R. Wang, D. Jia, Z. Wang, N. Lu, F. Ran and S. Peng, *Nano Res.*, 2022, **15**, 1942–1948.
12. L. Li, N. Li, J. Xia, S. Zhou, X. Qian, F. Yin, G. He and H. Chen, *Mater. Chem. A*, 2023, **11**, 2291–2301.
13. N. Meng, Y. Feng, Z. Zhao and F. Lian, *Small*, 2024, **20**, 2470260.
14. X. Han, X. Ling, Y. Wang, T. Ma, C. Zhong, W. Hu and Y. Deng, *Angew. Chem. Int. Ed.*, 2019, **58**, 5359–5364.
15. S. Zhang, Q. Zhou, L. Fang, R. Wang, T. Lu, Q. Zhao, X. Gu, S. Tian, L. Xu, H. Pang, J. Yang, Y. Tang and S. Sun, *App. Catal. B: Environ.*, 2023, **328**, 122489.
16. J. Rong, E. Gao, N. Liu, W. Chen, X. Rong, Y. Zhang, X. Zheng, H. Ao, S. Xue, B. Huang, Z. Li, F. Qiu and Y. Qian, *Energy Storage Mater.*, 2023, **56**, 165–173.
17. X. Han, X. Ling, D. Yu, D. Xie, L. Li, S. Peng, C. Zhong, N. Zhao, Y. Deng and W. Hu, *Adv. Mater.*, 2019, **31**, 1905622.
18. Y. Qi, Q. Liang, M. Wu, K. Song, M. Liu, Z. Jiang, X. Li, F. Yang and W. Zhang, *Nano Lett.*, 2025, **25**, 10690–10698.
19. W. Yao, A. Hu, J. Ding, N. Wang, Z. Qin, X. Yang, K. Shen, L. Chen and Y. Li, *Adv. Mater.*, 2023, **35**, 2301894.
20. Z. Zhang, X. Zhao, S. Xi, L. Zhang, Z. Chen, Z. Zeng, M. Huang, H. Yang, B. Liu, S. J. Pennycook and P. Chen, *Adv. Energy Mater.*, 2020, **10**, 2002896.
21. X. Wang, L. Xu, C. Li, C. Zhang, H. Yao, R. Xu, P. Cui, X. Zheng, M. Gu, J. Lee, H. Jiang and M. Huang, *Nat. Commun.*, 2023, **14**, 7210.
22. T. Sun, T. Li, D. Han, L. Liu and H.-g. Wang, *J. Electroanal. Chem.*, 2023, **928**, 117016.